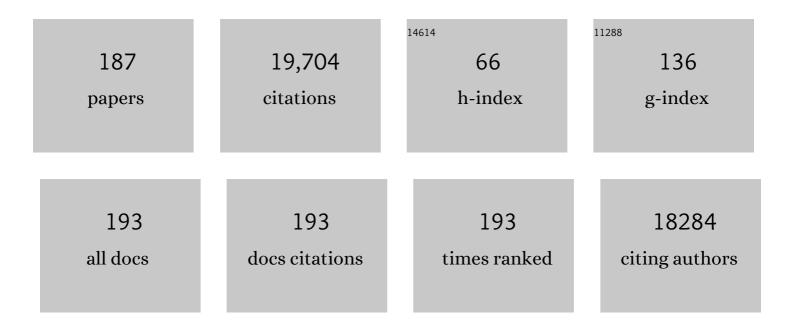
List of Publications by Year in descending order

Source: https://exaly.com/author-pdf/2531721/publications.pdf Version: 2024-02-01



Πονιςήλι Μεί

#	Article	IF	CITATIONS
1	Activation of surface lattice oxygen in single-atom Pt/CeO ₂ for low-temperature CO oxidation. Science, 2017, 358, 1419-1423.	6.0	1,114
2	Electrolyte additive enabled fast charging and stable cycling lithium metal batteries. Nature Energy, 2017, 2, .	19.8	1,048
3	Hierarchically Porous Graphene as a Lithium–Air Battery Electrode. Nano Letters, 2011, 11, 5071-5078.	4.5	943
4	Coordinatively Unsaturated Al ³⁺ Centers as Binding Sites for Active Catalyst Phases of Platinum on γ-Al ₂ O ₃ . Science, 2009, 325, 1670-1673.	6.0	790
5	Stable cycling of high-voltage lithium metal batteries in ether electrolytes. Nature Energy, 2018, 3, 739-746.	19.8	767
6	Highâ€Voltage Lithiumâ€Metal Batteries Enabled by Localized High oncentration Electrolytes. Advanced Materials, 2018, 30, e1706102.	11.1	761
7	Localized High-Concentration Sulfone Electrolytes for High-Efficiency Lithium-Metal Batteries. CheM, 2018, 4, 1877-1892.	5.8	628
8	Active Oxygen Vacancy Site for Methanol Synthesis from CO ₂ Hydrogenation on In ₂ O ₃ (110): A DFT Study. ACS Catalysis, 2013, 3, 1296-1306.	5.5	530
9	Self-smoothing anode for achieving high-energy lithium metal batteries under realistic conditions. Nature Nanotechnology, 2019, 14, 594-601.	15.6	451
10	Self-adaptive dual-metal-site pairs in metal-organic frameworks for selective CO2 photoreduction to CH4. Nature Catalysis, 2021, 4, 719-729.	16.1	406
11	Stabilization of Electrocatalytic Metal Nanoparticles at Metalâ^'Metal Oxideâ^'Graphene Triple Junction Points. Journal of the American Chemical Society, 2011, 133, 2541-2547.	6.6	391
12	Selective Catalytic Reduction over Cu/SSZ-13: Linking Homo- and Heterogeneous Catalysis. Journal of the American Chemical Society, 2017, 139, 4935-4942.	6.6	380
13	Dynamic formation of single-atom catalytic active sites on ceria-supported gold nanoparticles. Nature Communications, 2015, 6, 6511.	5.8	370
14	Insight into methanol synthesis from CO2 hydrogenation on Cu(111): Complex reaction network and the effects of H2O. Journal of Catalysis, 2011, 281, 199-211.	3.1	347
15	Dendrite-Free Lithium Deposition with Self-Aligned Nanorod Structure. Nano Letters, 2014, 14, 6889-6896.	4.5	326
16	High-Concentration Ether Electrolytes for Stable High-Voltage Lithium Metal Batteries. ACS Energy Letters, 2019, 4, 896-902.	8.8	302
17	Toward Rational Design of Cu/SSZ-13 Selective Catalytic Reduction Catalysts: Implications from Atomic-Level Understanding of Hydrothermal Stability. ACS Catalysis, 2017, 7, 8214-8227.	5.5	278
18	Mechanistic studies of methanol synthesis over Cu from CO/CO2/H2/H2O mixtures: The source of C in methanol and the role of water. Journal of Catalysis, 2013, 298, 10-17.	3.1	271

#	Article	IF	CITATIONS
19	Hierarchical Porous NC@CuCo Nitride Nanosheet Networks: Highly Efficient Bifunctional Electrocatalyst for Overall Water Splitting and Selective Electrooxidation of Benzyl Alcohol. Advanced Functional Materials, 2017, 27, 1704169.	7.8	267
20	Hydrogenation of acetylene–ethylene mixtures over Pd and Pd–Ag alloys: First-principles-based kinetic Monte Carlo simulations. Journal of Catalysis, 2009, 268, 181-195.	3.1	256
21	Highly Stable Operation of Lithium Metal Batteries Enabled by the Formation of a Transient High oncentration Electrolyte Layer. Advanced Energy Materials, 2016, 6, 1502151.	10.2	236
22	First-Principles Study of Phenol Hydrogenation on Pt and Ni Catalysts in Aqueous Phase. Journal of the American Chemical Society, 2014, 136, 10287-10298.	6.6	226
23	Controlling Solid–Liquid Conversion Reactions for a Highly Reversible Aqueous Zinc–lodine Battery. ACS Energy Letters, 2017, 2, 2674-2680.	8.8	207
24	Quantitatively Probing the Al Distribution in Zeolites. Journal of the American Chemical Society, 2014, 136, 8296-8306.	6.6	199
25	Methanol synthesis from CO2 hydrogenation over a Pd4/In2O3 model catalyst: A combined DFT and kinetic study. Journal of Catalysis, 2014, 317, 44-53.	3.1	196
26	Enhanced charging capability of lithium metal batteries based on lithium bis(trifluoromethanesulfonyl)imide-lithium bis(oxalato)borate dual-salt electrolytes. Journal of Power Sources, 2016, 318, 170-177.	4.0	186
27	First-principles-based kinetic Monte Carlo simulation of the selective hydrogenation of acetylene over Pd(111). Journal of Catalysis, 2006, 242, 1-15.	3.1	178
28	Ethanol synthesis from syngas over Rh-based/SiO2 catalysts: A combined experimental and theoretical modeling study. Journal of Catalysis, 2010, 271, 325-342.	3.1	174
29	Single-Atom Pt–N ₃ Sites on the Stable Covalent Triazine Framework Nanosheets for Photocatalytic N ₂ Fixation. ACS Catalysis, 2020, 10, 2431-2442.	5.5	171
30	Stable platinum nanoparticles on specific MgAl2O4 spinel facets at high temperatures in oxidizing atmospheres. Nature Communications, 2013, 4, 2481.	5.8	166
31	Liquid-metal electrode to enable ultra-low temperature sodium–beta alumina batteries for renewable energy storage. Nature Communications, 2014, 5, 4578.	5.8	158
32	Graphene Oxide Catalyzed Câ^'H Bond Activation: The Importance of Oxygen Functional Groups for Biaryl Construction. Angewandte Chemie - International Edition, 2016, 55, 3124-3128.	7.2	129
33	Reduction Mechanism of Fluoroethylene Carbonate for Stable Solid–Electrolyte Interphase Film on Silicon Anode. ChemSusChem, 2014, 7, 549-554.	3.6	126
34	Mechanisms of catalytic cleavage of benzyl phenyl ether in aqueous and apolar phases. Journal of Catalysis, 2014, 311, 41-51.	3.1	120
35	Effects of La ₂ O ₃ on the Mixed Higher Alcohols Synthesis from Syngas over Co Catalysts: A Combined Theoretical and Experimental Study. Journal of Physical Chemistry C, 2011, 115, 17440-17451.	1.5	119
36	Genesis and Stability of Hydronium Ions in Zeolite Channels. Journal of the American Chemical Society, 2019, 141, 3444-3455.	6.6	119

#	Article	IF	CITATIONS
37	Effects of Hydration and Oxygen Vacancy on CO ₂ Adsorption and Activation on β-Ga ₂ O ₃ (100). Langmuir, 2010, 26, 5551-5558.	1.6	118
38	Effect of the Anion Activity on the Stability of Li Metal Anodes in Lithium‣ulfur Batteries. Advanced Functional Materials, 2016, 26, 3059-3066.	7.8	117
39	Promotional effect of surface hydroxyls on electrochemical reduction of CO2 over SnO /Sn electrode. Journal of Catalysis, 2016, 343, 257-265.	3.1	113
40	Dehydration Pathways of 1-Propanol on HZSM-5 in the Presence and Absence of Water. Journal of the American Chemical Society, 2015, 137, 15781-15794.	6.6	110
41	Effects of Imide–Orthoborate Dual-Salt Mixtures in Organic Carbonate Electrolytes on the Stability of Lithium Metal Batteries. ACS Applied Materials & Interfaces, 2018, 10, 2469-2479.	4.0	110
42	Mechanisms of selective cleavage of C–O bonds in di-aryl ethers in aqueous phase. Journal of Catalysis, 2014, 309, 280-290.	3.1	108
43	Highly Active Ir/In ₂ O ₃ Catalysts for Selective Hydrogenation of CO ₂ to Methanol: Experimental and Theoretical Studies. ACS Catalysis, 2021, 11, 4036-4046.	5.5	108
44	Key Roles of Lewis Acid–Base Pairs on Zn _{<i>x</i>} Zr _{<i>y</i>} O _{<i>z</i>} in Direct Ethanol/Acetone to Isobutene Conversion. Journal of the American Chemical Society, 2016, 138, 507-517.	6.6	106
45	Potential Energy Surface of Methanol Decomposition on Cu(110). Journal of Physical Chemistry C, 2009, 113, 4522-4537.	1.5	105
46	(100) facets of Î ³ -Al2O3: The Active Surfaces for Alcohol Dehydration Reactions. Catalysis Letters, 2011, 141, 649-655.	1.4	105
47	Morphology controlled synthesis of α-Fe2O3-x with benzimidazole-modified Fe-MOFs for enhanced photo-Fenton-like catalysis. Applied Catalysis B: Environmental, 2021, 291, 120129.	10.8	105
48	Highly active and stable MgAl2O4-supported Rh and Ir catalysts for methane steam reforming: A combined experimental and theoretical study. Journal of Catalysis, 2014, 316, 11-23.	3.1	104
49	Enhanced Cycling Stability of Rechargeable Li–O ₂ Batteries Using High oncentration Electrolytes. Advanced Functional Materials, 2016, 26, 605-613.	7.8	104
50	Unique Role of Anchoring Penta-Coordinated Al ³⁺ Sites in the Sintering of γ-Al ₂ O ₃ -Supported Pt Catalysts. Journal of Physical Chemistry Letters, 2010, 1, 2688-2691.	2.1	101
51	Stabilization of Li Metal Anode in DMSOâ€Based Electrolytes via Optimization of Salt–Solvent Coordination for Li–O ₂ Batteries. Advanced Energy Materials, 2017, 7, 1602605.	10.2	99
52	Unraveling the mysterious failure of Cu/SAPO-34 selective catalytic reduction catalysts. Nature Communications, 2019, 10, 1137.	5.8	99
53	Enhancing the catalytic activity of hydronium ions through constrained environments. Nature Communications, 2017, 8, 14113.	5.8	94
54	Functionalized Graphene Sheets as Molecular Templates for Controlled Nucleation and Selfâ€Assembly of Metal Oxideâ€Graphene Nanocomposites. Advanced Materials, 2012, 24, 5136-5141.	11.1	92

#	Article	IF	CITATIONS
55	Experimental and Modeling Studies on the Hydrate Formation of a Methane + Nitrogen Gas Mixture in the Presence of Aqueous Electrolyte Solutions. Industrial & Engineering Chemistry Research, 1996, 35, 4342-4347.	1.8	89
56	Metal-organic framework encapsulated single-atom Pt catalysts for efficient photocatalytic hydrogen evolution. Journal of Catalysis, 2019, 375, 351-360.	3.1	86
57	DFT+U Study on the Localized Electronic States and Their Potential Role During H ₂ O Dissociation and CO Oxidation Processes on CeO ₂ (111) Surface. Journal of Physical Chemistry C, 2013, 117, 23082-23089.	1.5	85
58	Ultrathin Lowâ€Crystallinity MOF Membranes Fabricated by Interface Layer Polarization Induction. Advanced Materials, 2020, 32, e2002165.	11.1	85
59	Ethylene Hydrogenation over Bimetallic Pd/Au(111) Surfaces:  Application of Quantum Chemical Results and Dynamic Monte Carlo Simulation. Journal of Physical Chemistry B, 2003, 107, 798-810.	1.2	82
60	Understanding the nature of surface nitrates in BaO/ $\hat{1}^3$ -Al2O3 NOx storage materials: A combined experimental and theoretical study. Journal of Catalysis, 2009, 261, 17-22.	3.1	79
61	Promotional Effects of Cesium Promoter on Higher Alcohol Synthesis from Syngas over Cesium-Promoted Cu/ZnO/Al ₂ O ₃ Catalysts. ACS Catalysis, 2016, 6, 5771-5785.	5.5	79
62	Surface-Bound Intermediates in Low-Temperature Methanol Synthesis on Copper: Participants and Spectators. ACS Catalysis, 2015, 5, 7328-7337.	5.5	77
63	Size-Dependent Catalytic Performance of CuO on γ-Al ₂ O ₃ : NO Reduction versus NH ₃ Oxidation. ACS Catalysis, 2012, 2, 1432-1440.	5.5	75
64	Metal-Free 2D/2D Black Phosphorus and Covalent Triazine Framework Heterostructure for CO ₂ Photoreduction. ACS Sustainable Chemistry and Engineering, 2020, 8, 5175-5183.	3.2	74
65	Tracking the Chemical Transformations at the BrÃ,nsted Acid Site upon Water-Induced Deprotonation in a Zeolite Pore. Chemistry of Materials, 2017, 29, 9030-9042.	3.2	71
66	Entrapped Single Tungstate Site in Zeolite for Cooperative Catalysis of Olefin Metathesis with BrÃ,nsted Acid Site. Journal of the American Chemical Society, 2018, 140, 6661-6667.	6.6	71
67	New insights into reaction mechanisms of ethanol steam reforming on Co–ZrO2. Applied Catalysis B: Environmental, 2015, 162, 141-148.	10.8	67
68	Hydrate Formation of a Synthetic Natural Gas Mixture in Aqueous Solutions Containing Electrolyte, Methanol, and (Electrolyte + Methanol). Journal of Chemical & Engineering Data, 1998, 43, 178-182.	1.0	66
69	Ethylene conversion to ethylidyne on Pd(111) and Pt(111): A first-principles-based kinetic Monte Carlo study. Journal of Catalysis, 2012, 285, 187-195.	3.1	66
70	Mechanisms of Semiconducting 2H to Metallic 1T Phase Transition in Two-dimensional MoS ₂ Nanosheets. Journal of Physical Chemistry C, 2018, 122, 28215-28224.	1.5	65
71	Density Functional Theory Study of Acetaldehyde Hydrodeoxygenation on MoO ₃ . Journal of Physical Chemistry C, 2011, 115, 8155-8164.	1.5	64
72	Synergistic Effect of Nitrogen in Cobalt Nitride and Nitrogenâ€Doped Hollow Carbon Spheres for the Oxygen Reduction Reaction. ChemCatChem, 2015, 7, 1826-1832.	1.8	62

#	Article	IF	CITATIONS
73	Hydrogen Adsorption on Ga ₂ O ₃ Surface: A Combined Experimental and Computational Study. Journal of Physical Chemistry C, 2011, 115, 10140-10146.	1.5	61
74	Adaptive kinetic Monte Carlo simulation of methanol decomposition on Cu(100). Journal of Chemical Physics, 2009, 131, 244520.	1.2	59
75	Revisiting effects of alkali metal and alkaline earth co-cation additives to Cu/SSZ-13 selective catalytic reduction catalysts. Journal of Catalysis, 2019, 378, 363-375.	3.1	59
76	From first principles to catalytic performance: tracking molecular transformations. Chemical Engineering Science, 2004, 59, 4703-4714.	1.9	58
77	Following Solidâ€Acidâ€Catalyzed Reactions by MAS NMR Spectroscopy in Liquid Phase—Zeoliteâ€Catalyzed Conversion of Cyclohexanol in Water. Angewandte Chemie - International Edition, 2014, 53, 479-482.	7.2	57
78	Methanol Adsorption on the Clean CeO2(111) Surface:  A Density Functional Theory Study. Journal of Physical Chemistry C, 2007, 111, 10514-10522.	1.5	56
79	Mechanism of Phenol Alkylation in Zeolite H-BEA Using In Situ Solid-State NMR Spectroscopy. Journal of the American Chemical Society, 2017, 139, 9178-9185.	6.6	56
80	Simultaneous Activation of CH ₄ and CO ₂ for Concerted C–C Coupling at Oxide–Oxide Interfaces. ACS Catalysis, 2019, 9, 3187-3197.	5.5	56
81	Mechanistic insight into the passive NOx adsorption in the highly dispersed Pd/HBEA zeolite. Applied Catalysis A: General, 2019, 569, 181-189.	2.2	55
82	Adsorption of Potassium on MoS ₂ (100) Surface: A First-Principles Investigation. Journal of Physical Chemistry C, 2011, 115, 9025-9040.	1.5	54
83	A General Mechanism for Stabilizing the Small Sizes of Precious Metal Nanoparticles on Oxide Supports. Chemistry of Materials, 2014, 26, 5475-5481.	3.2	53
84	Mechanistic insights into the structureâ€dependent selectivity of catalytic furfural conversion on platinum catalysts. AICHE Journal, 2015, 61, 3812-3824.	1.8	53
85	Dimer saddle point searches to determine the reactivity of formate on Cu(111). Journal of Catalysis, 2008, 258, 44-51.	3.1	51
86	Synergistic effect of the metal-support interaction and interfacial oxygen vacancy for CO2 hydrogenation to methanol over Ni/In2O3 catalyst: A theoretical study. Journal of Energy Chemistry, 2022, 65, 623-629.	7.1	51
87	Unveiling Secondary-Ion-Promoted Catalytic Properties of Cu-SSZ-13 Zeolites for Selective Catalytic Reduction of NO <i>_x</i> . Journal of the American Chemical Society, 2022, 144, 12816-12824.	6.6	51
88	First-principles-based kinetic Monte Carlo simulation of nitric oxide decomposition over Pt and Rh surfaces under lean-burn conditions. Molecular Physics, 2004, 102, 361-369.	0.8	50
89	First-Principles Characterization of Potassium Intercalation in Hexagonal 2H-MoS ₂ . Journal of Physical Chemistry C, 2012, 116, 1826-1832.	1.5	50
90	Mechanistic Effects of Water on the Fe-Catalyzed Hydrodeoxygenation of Phenol. The Role of BrĄ̃,nsted Acid Sites. ACS Catalysis, 2018, 8, 2200-2208.	5.5	50

#	Article	IF	CITATIONS
91	Screening by Kinetic Monte Carlo Simulation of Ptâ du(100) Surfaces for the Steady-State Decomposition of Nitric Oxide in Excess Dioxygenâ€. Journal of Physical Chemistry B, 2005, 109, 2234-2244.	1.2	49
92	Mechanistic insights into aqueous phase propanol dehydration in Hâ€ZSMâ€5 zeolite. AICHE Journal, 2017, 63, 172-184.	1.8	49
93	Title is missing!. Topics in Catalysis, 2002, 20, 5-23.	1.3	47
94	Hydrolysis of zeolite framework aluminum and its impact on acid catalyzed alkane reactions. Journal of Catalysis, 2018, 365, 359-366.	3.1	47
95	Isotope Effects in Methanol Synthesis and the Reactivity of Copper Formates on a Cu/SiO2 Catalyst. Catalysis Letters, 2008, 125, 201-208.	1.4	46
96	The OH ^{â^'} -driven synthesis of Pt–Ni nanocatalysts with atomic segregation for alkaline hydrogen evolution reaction. Journal of Materials Chemistry A, 2019, 7, 5475-5481.	5.2	46
97	Theoretical Study of Syngas Hydrogenation to Methanol on the Polar Zn-Terminated ZnO(0001) Surface. Journal of Physical Chemistry C, 2012, 116, 15952-15961.	1.5	45
98	Steam Reforming of Ethylene Glycol over MgAl ₂ O ₄ Supported Rh, Ni, and Co Catalysts. ACS Catalysis, 2016, 6, 315-325.	5.5	45
99	Polymer-supported ultra-thin ZIF-67 membrane through in situ interface self-repair. Journal of Membrane Science, 2021, 625, 119139.	4.1	45
100	A density functional theory study of formaldehyde adsorption on ceria. Surface Science, 2007, 601, 4993-5001.	0.8	44
101	Effects of cell positive cans and separators on the performance of high-voltage Li-ion batteries. Journal of Power Sources, 2012, 213, 160-168.	4.0	44
102	Constructing Robust Electrode/Electrolyte Interphases to Enable Wide Temperature Applications of Lithium-Ion Batteries. ACS Applied Materials & Interfaces, 2019, 11, 21496-21505.	4.0	44
103	Reversible Electrochemical Interface of Mg Metal and Conventional Electrolyte Enabled by Intermediate Adsorption. ACS Energy Letters, 2020, 5, 200-206.	8.8	44
104	State of Supported Pd during Catalysis in Water. Journal of Physical Chemistry C, 2013, 117, 17603-17612.	1.5	43
105	Density Functional Theory Study of Methanol Decomposition on the CeO2(110) Surface. Journal of Physical Chemistry C, 2008, 112, 4257-4266.	1.5	42
106	The Role of Cesium Cation in Controlling Interphasial Chemistry on Graphite Anode in Propylene Carbonate-Rich Electrolytes. ACS Applied Materials & Interfaces, 2015, 7, 20687-20695.	4.0	41
107	Effects of Local Water Concentrations on Cyclohexanol Dehydration in H-BEA Zeolites. Journal of Physical Chemistry C, 2019, 123, 25255-25266.	1.5	40
108	The Critical Role of Reductive Steps in the Nickel atalyzed Hydrogenolysis and Hydrolysis of Aryl Ether Câ^'O Bonds. Angewandte Chemie - International Edition, 2020, 59, 1445-1449.	7.2	40

#	Article	IF	CITATIONS
109	Adsorption and diffusion of a single Pt atom on \hat{I}^3 -Al2O3 surfaces. Surface Science, 2009, 603, 2793-2807.	0.8	39
110	Comparative Investigation of Benzene Steam Reforming over Spinel Supported Rh and Ir Catalysts. ACS Catalysis, 2013, 3, 1133-1143.	5.5	39
111	First-Principles Thermodynamics Study of Spinel MgAl ₂ O ₄ Surface Stability. Journal of Physical Chemistry C, 2016, 120, 19087-19096.	1.5	38
112	First-Principles-Based Kinetic Monte Carlo Simulation of Nitric Oxide Reduction over Platinum Nanoparticles under Lean-Burn Conditions. Industrial & Engineering Chemistry Research, 2010, 49, 10364-10373.	1.8	36
113	Copper Phyllosilicate Nanotube Catalysts for the Chemosynthesis of Cyclohexane via Hydrodeoxygenation of Phenol. ACS Catalysis, 2022, 12, 4724-4736.	5.5	35
114	Minimizing the Formation of Coke and Methane on Co Nanoparticles in Steam Reforming of Biomassâ€Derived Oxygenates. ChemCatChem, 2013, 5, 1299-1303.	1.8	34
115	Vapor Phase Ketonization of Acetic Acid on Ceria Based Metal Oxides. Topics in Catalysis, 2013, 56, 1782-1789.	1.3	33
116	Multifunctional Pd-Sn electrocatalysts enabled by in situ formed SnOx and TiC triple junctions. Nano Energy, 2018, 53, 940-948.	8.2	33
117	Aqueous-Phase Acetic Acid Ketonization over Monoclinic Zirconia. ACS Catalysis, 2018, 8, 488-502.	5.5	32
118	Single-Facet Dominant Anatase TiO ₂ (101) and (001) Model Catalysts to Elucidate the Active Sites for Alkanol Dehydration. ACS Catalysis, 2020, 10, 4268-4279.	5.5	32
119	Reactivity of hydrogen and methanol on (001) surfaces of WO3, ReO3, WO3/ReO3 and ReO3/WO3. Catalysis Today, 2011, 165, 41-48.	2.2	31
120	The Origin of Regioselectivity in 2â€Butanol Dehydration on Solid Acid Catalysts. ChemCatChem, 2011, 3, 1557-1561.	1.8	30
121	Theoretical Insights into the Initial Hydrolytic Breakdown of HKUST-1. Journal of Physical Chemistry C, 2020, 124, 1991-2001.	1.5	30
122	Adsorption and Formation of BaO Overlayers on γ-Al ₂ O ₃ Surfaces. Journal of Physical Chemistry C, 2008, 112, 18050-18060.	1.5	29
123	Stable and size-controllable ultrafine Pt nanoparticles derived from a MOF-based single metal ion trap for efficient electrocatalytic hydrogen evolution. Journal of Materials Chemistry A, 2019, 7, 20239-20246.	5.2	29
124	First-Principles Analysis of NO _{<i>x</i>} Adsorption on Anhydrous γ-Al ₂ O ₃ Surfaces. Journal of Physical Chemistry C, 2009, 113, 7779-7789.	1.5	28
125	Structure sensitivity of hydrogenolytic cleavage of endocyclic and exocyclic C–C bonds in methylcyclohexane over supported iridium particles. Journal of Catalysis, 2013, 297, 70-78.	3.1	28
126	Size-dependent electron injection over sensitized semiconductor heterojunctions for enhanced photocatalytic hydrogen production. Applied Catalysis B: Environmental, 2022, 308, 121218.	10.8	28

#	Article	IF	CITATIONS
127	Covalent triazine framework encapsulated Pd nanoclusters for efficient hydrogen production via ammonia borane hydrolysis. Journal of Catalysis, 2022, 411, 72-83.	3.1	27
128	Theoretical Investigation of the Structural Stabilities of Ceria Surfaces and Supported Metal Nanocluster in Vapor and Aqueous Phases. Journal of Physical Chemistry C, 2018, 122, 4828-4840.	1.5	26
129	Elucidation of Active Sites in Aldol Condensation of Acetone over Single-Facet Dominant Anatase TiO ₂ (101) and (001) Catalysts. Jacs Au, 2021, 1, 41-52.	3.6	26
130	Steam Reforming of Acetic Acid over Co-Supported Catalysts: Coupling Ketonization for Greater Stability. ACS Sustainable Chemistry and Engineering, 2017, 5, 9136-9149.	3.2	25
131	A theoretical study on reaction mechanisms and kinetics of thiophene hydrodesulfurization over MoS2 catalysts. Catalysis Today, 2018, 312, 158-167.	2.2	25
132	Distinct Role of Surface Hydroxyls in Single-Atom Pt ₁ /CeO ₂ Catalyst for Room-Temperature Formaldehyde Oxidation: Acid–Base Versus Redox. Jacs Au, 2022, 2, 1651-1660.	3.6	25
133	Structure H clathrate unit cell coordinates and simulation of the structure H crystal interface with water. Journal of Chemical Physics, 1997, 106, 4187-4195.	1.2	24
134	Hydronium-Ion-Catalyzed Elimination Pathways of Substituted Cyclohexanols in Zeolite H-ZSM5. ACS Catalysis, 2017, 7, 7822-7829.	5.5	22
135	In Situ Fabrication of PtCo Alloy Embedded in Nitrogenâ€Doped Graphene Nanopores as Synergistic Catalyst for Oxygen Reduction Reaction. Advanced Materials Interfaces, 2015, 2, 1500365.	1.9	21
136	Identifying Free Energy Landscapes of Proton-Transfer Processes between BrÃ,nsted Acid Sites and Water Clusters Inside the Zeolite Pores. Journal of Physical Chemistry C, 2020, 124, 22568-22576.	1.5	20
137	Water: A promoter of ammonia selective catalytic reduction over copper-exchanged LTA zeolites. Applied Catalysis B: Environmental, 2021, 294, 120244.	10.8	20
138	Effects of potassium doping on CO hydrogenation over MoS2 catalysts: A first-principles investigation. Catalysis Communications, 2014, 52, 92-97.	1.6	19
139	Theoretical Insights into CO Oxidation over MOF-808-Encapsulated Single-Atom Metal Catalysts. Journal of Physical Chemistry C, 2021, 125, 17097-17108.	1.5	19
140	Effects of heat and mass transfer on the kinetics of CO oxidation over RuO2(110) catalyst. Catalysis Today, 2011, 165, 56-63.	2.2	18
141	A radar-like iron based nanohybrid as an efficient and stable electrocatalyst for oxygen reduction. Journal of Materials Chemistry A, 2014, 2, 6703-6707.	5.2	18
142	Dynamic modification of pore opening of SAPO-34 by adsorbed surface methoxy species during induction of catalytic methanol-to-olefins reactions. Applied Catalysis B: Environmental, 2018, 237, 245-250.	10.8	18
143	Prediction of Gas Hydrate Formation Conditions in Aqueous Solutions Containing Electrolytes and (Electrolytes + Methanol). Industrial & Engineering Chemistry Research, 1999, 38, 1700-1705.	1.8	17
144	On the Reaction Mechanism of Acetaldehyde Decomposition on Mo(110). ACS Catalysis, 2012, 2, 468-478.	5.5	16

#	Article	IF	CITATIONS
145	Dehydration of 1-Octadecanol over H-BEA: A Combined Experimental and Computational Study. ACS Catalysis, 2016, 6, 878-889.	5.5	16
146	Nucleation of Cu <i>_n</i> (<i>n</i> = 1–5) Clusters and Equilibrium Morphology of Cu Particles Supported on CeO ₂ Surface: A Density Functional Theory Study. Journal of Physical Chemistry C, 2018, 122, 27402-27411.	1.5	15
147	Aqueous Phase Aldol Condensation of Formaldehyde and Acetone on Anatase TiO ₂ (101) Surface: A Theoretical Investigation. ChemCatChem, 2020, 12, 1220-1229.	1.8	15
148	Adsorption Kinetics in Nanoscale Porous Coordination Polymers. ACS Applied Materials & amp; Interfaces, 2015, 7, 21712-21716.	4.0	14
149	A combined experimental and computational study of water-gas shift reaction over rod-shaped Ce0.75M0.25O2 (M = Ti, Zr, and Mn) supported Cu catalysts. International Journal of Hydrogen Energy, 2017, 42, 30086-30097.	3.8	14
150	The Role of Ir in Ternary Rh-Based Catalysts for Syngas Conversion to C2 + Oxygenates. Topics in Catalysis, 2012, 55, 595-600.	1.3	13
151	Effect of graphene with nanopores on metal clusters. Physical Chemistry Chemical Physics, 2015, 17, 24420-24426.	1.3	13
152	Hydrogen assisted synthesis of branched nickel nanostructures: a combined theoretical and experimental study. Physical Chemistry Chemical Physics, 2017, 19, 26718-26727.	1.3	13
153	<scp>Airâ€Steam</scp> Etched Construction of Hierarchically Porous <scp>Metalâ€Organic</scp> Frameworks. Chinese Journal of Chemistry, 2021, 39, 1538-1544.	2.6	13
154	First-principles characterization of formate and carboxyl adsorption on stoichiometric CeO2(111) and CeO2(110) surfaces. Journal of Energy Chemistry, 2013, 22, 524-532.	7.1	12
155	Monitoring the methanol conversion process in H-ZSM-5 using synchrotron X-ray powder diffraction-mass spectrometry. Journal of Catalysis, 2018, 365, 145-152.	3.1	12
156	A comparative study of the adsorption of water and methanol in zeolite BEA: a molecular simulation study. Molecular Simulation, 2014, 40, 1113-1124.	0.9	11
157	Geometric and electronic properties of graphene modified by "external―N-containing groups. Physical Chemistry Chemical Physics, 2014, 16, 20749-20754.	1.3	11
158	Structural and Hydrolytic Stability of Coordinatively Unsaturated Metal–Organic Frameworks M ₃ (BTC) ₂ (M = Cu, Co, Mn, Ni, and Zn): A Combined DFT and Experimental Study. Journal of Physical Chemistry C, 2021, 125, 5832-5847.	1.5	11
159	Characterization of surface and bulk nitrates of γ-Al2O3–supported alkaline earth oxides using density functional theory. Physical Chemistry Chemical Physics, 2009, 11, 3380.	1.3	10
160	Density Functional Theory Study of Surface Carbonate Formation on BaO(001). Journal of Physical Chemistry C, 2010, 114, 1867-1874.	1.5	10
161	Artificial Neural Network Potential for Encapsulated Platinum Clusters in MOF-808. Journal of Physical Chemistry C, 2022, 126, 1204-1214.	1.5	10
162	A DFT+U study of structure and reducibility of CenO2nâ^'x (n⩽4, 0⩽x⩽n) nanoclusters. Computation Theoretical Chemistry, 2012, 987, 25-31	al and	9

Theoretical Chemistry, 2012, 987, 25-31.

#	Article	IF	CITATIONS
163	Rational Design of Synergistic Active Sites for Catalytic Ethene/2-Butene Cross-Metathesis in a Rhenium-Doped Y Zeolite Catalyst. ACS Catalysis, 2021, 11, 3530-3540.	5.5	9
164	Catalyst size and morphological effects on the interaction of NO2 with BaO/ \hat{I}^3 -Al2O3 materials. Catalysis Today, 2010, 151, 304-313.	2.2	8
165	Competitive Adsorption-Assisted Formation of One-Dimensional Cobalt Nanochains with High CO Hydrogenation Activity. Journal of Physical Chemistry C, 2017, 121, 24588-24593.	1.5	8
166	Quasi-Solid-State Li–O ₂ Batteries Performance Enhancement Using an Integrated Composite Polymer-Based Architecture. ACS Applied Energy Materials, 2021, 4, 6221-6232.	2.5	8
167	Copper-Based Catalysts Confined in Carbon Nanocage Reactors for Condensed Ester Hydrogenation: Tuning Copper Species by Confined SiO ₂ and Methanol Resistance. ACS Sustainable Chemistry and Engineering, 2021, 9, 16270-16280.	3.2	8
168	Mechanistic understanding of methane combustion over H-SSZ-13 zeolite encapsulated palladium nanocluster catalysts. Chemical Engineering Journal, 2022, 444, 136671.	6.6	8
169	Origin of Support Effects on the Reactivity of a Ceria Cluster. Journal of Physical Chemistry C, 2009, 113, 18296-18303.	1.5	7
170	Isomeric Li–La–Zr–O Amorphous–Crystalline Composite Thin-Film Electrolytes for All-Solid-State Lithium Batteries. ACS Applied Energy Materials, 2021, 4, 8517-8528.	2.5	7
171	Formation, Characterization, and Reactivity of Adsorbed Oxygen on BaO/Pt(111). Journal of Physical Chemistry C, 2010, 114, 20195-20206.	1.5	6
172	The Critical Role of Reductive Steps in the Nickelâ€Catalyzed Hydrogenolysis and Hydrolysis of Aryl Ether Câ^'O Bonds. Angewandte Chemie, 2020, 132, 1461-1465.	1.6	6
173	A density functional theoretical study on the stability of Pt clusters in MOF-808. Physical Chemistry Chemical Physics, 2020, 22, 23645-23656.	1.3	6
174	Density Functional Theory Study on the Morphology Evolution of Hydroxylated Î ² -Cristobalite Silica and Desilication in the Presence of Methanol. Journal of Physical Chemistry C, 2021, 125, 7868-7879.	1.5	6
175	A theoretical study of propionic acid decarboxylation over hydroxyapatite supported platinum catalysts. Catalysis Today, 2021, 365, 181-192.	2.2	6
176	Dealumination of the H-BEA Zeolite via the <i>S</i> _{N2} Mechanism: A Theoretical Investigation. Journal of Physical Chemistry C, 2021, 125, 24613-24621.	1.5	6
177	Understanding the Effects of Water Molecules on Cyclohexanol Dehydration over Zeolitic Acid Sites. Journal of Physical Chemistry C, 2021, 125, 15283-15291.	1.5	5
178	Theoretical characterization of zeolite encapsulated platinum clusters in the presence of water molecules. Physical Chemistry Chemical Physics, 2021, 23, 23360-23371.	1.3	5
179	Lithiumâ€Metal Batteries: Highâ€Voltage Lithiumâ€Metal Batteries Enabled by Localized Highâ€Concentration Electrolytes (Adv. Mater. 21/2018). Advanced Materials, 2018, 30, 1870144.	11.1	4
180	Insights into protonation for cyclohexanol/water mixtures at the zeolitic BrÃ,nsted acid site. Physical Chemistry Chemical Physics, 2021, 23, 10395-10401.	1.3	4

#	Article	IF	CITATIONS
181	Solarâ€Boosted Paperâ€Based Microfluidic Fuel Cells for Miniaturized Power Sources. Advanced Materials Technologies, 2022, 7, .	3.0	4
182	Molecular Dynamics Simulations of Model Perhydrogenated and Perfluorinated Alkyl Chains, Droplets, and Micelles. Langmuir, 2002, 18, 9067-9079.	1.6	3
183	Where Does the Sulphur Go? Deactivation of a Low Temperature CO Oxidation Catalyst by Sulphur Poisoning. Catalysis Letters, 2018, 148, 1445-1450.	1.4	3
184	The shuttling mechanism of foldaxanes: more than just translocation and rotation. Physical Chemistry Chemical Physics, 2020, 22, 12967-12972.	1.3	3
185	Thermodynamic and kinetic roles of H2 in structure evolution of urchin-like Co: A density functional theory study. Particuology, 2020, 48, 2-12.	2.0	2
186	Effects of hydroxylation on the acidic and basic strengths of anatase TiO ₂ surfaces. Molecular Simulation, 2022, 48, 829-843.	0.9	2
187	CO Oxidation over HKUST-1 Catalysts: The Role of Defective Sites. Journal of Physical Chemistry C, 2022, 126, 9652-9664.	1.5	2